Acta of Bioengineering and Biomechanics
Vol. 4, No. 1, 2002

Modelling of heat transfer in biomechanics – a review Part I. Soft tissues

M. STAŃCZYK, J.J. TELEGA

Polish Academy of Sciences, Institute of Fundamental Technological Research,
ul. Świętokrzyska 21, 00-049 Warsaw, Poland. E-mail: mstan@ippt.gov.pl, jtelega@ippt.gov.pl

The aim of this paper is to review available results that pertain to various heat transfer problems of biomechanics. The present part covers the issues connected with modelling of the heat exchange in perfused tissues. The results are important for the design of hyperthermic treatment protocols, thermal injury assessment, heat loss rate in adverse environments, constructing whole-body or whole-limb models of heat transfer, etc. The division into two classes of models is proposed: continuum models and vascular models (cf. also [[3]]). The shortcomings of the most popular bioheat transfer equations are discussed.

The effects of cryogenic temperatures on living tissues are described in the third part of the paper.

Key words: heat transfer models, continuum models, vascular models, perfused tissues

1. Introduction

Comprehension of phenomenon of heat transfer due to blood perfusion in soft tissues is important for all considerations of heat exchange in such tissues for various reasons. It helps to predict the outcome of modern surgical treatments involving local application of high temperature to diseased tissue. Heat sources include fiber optics coupled to Nd:YAG (neodymium–yttrium–aluminium–garnet) lasers, microwave antennas, radio-frequency transducers, ultrasound emitters, Joule-heated probes, saline-filled balloons and others. It is necessary for constructing whole-body or whole-limb heat transfer models that can be used for various practical purposes like predicting heat loss rate in water, wind cooling, thermoregulation efficacy etc., cf. [50]. Modelling of heat transfer in soft tissues is also necessary for an accurate assessment of energy dissipation rate in joints and for thermal analysis of the first stages of cryosurgical protocols (before freezing when effects of blood circulation are observed). The problems presented here are therefore inevitably linked with the issues presented in the remaining parts of the paper.

One of the most important purposes of the modelling of heat transfer in living tissues is to be able to predict the level and the area of potential damage caused by extreme

temperature to tissues. In the first part of our paper, the issues concerning damage to soft tissues caused by hyperthermia are briefly discussed. For a review of damage mechanisms due to low temperatures the reader is referred to Part III of the present paper.

2. Modelling of heat exchange in perfused tissues

Heat transport in living soft tissues is supplemented with one important factor not present in *in vitro* experiments, namely the vascularity. It needs to be taken into account in certain problems, while it can be omitted in others with only a slight penalty in accuracy. The procedure usually applied during modelling of the heat transfer in soft tissues is schematically depicted in figure1. Numerous phenomena of heat deposition (surface convection, irradiation, Joule heat generation etc.) along with analytical and numerical results for different boundary conditions are discussed at length in [21]. Here, we focus on the proposed forms of the *bioheat equation* which plays an important role in the modelling process, as shown in figure 1.

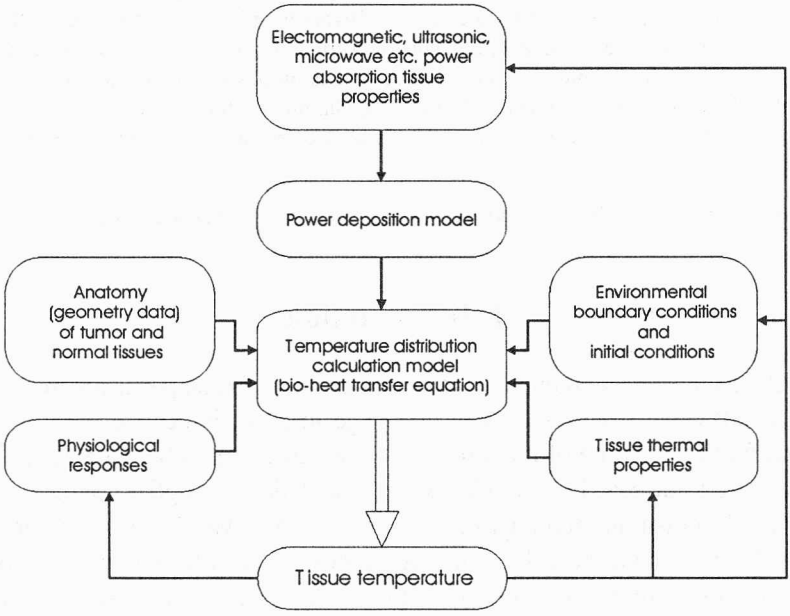

Fig. 1. Steps involved in the modelling of heat transfer (e.g. during hyperthermia treatment) in soft tissues

Theoretical analysis of the heat transport in soft tissues has been an object of an intense research. The models proposed can be basically divided into two categories (cf. BAISH et al. [3]): vascular and continuum models. The former try to reproduce the real vascularity of the tissue and to describe all local variations of the temperature

near the individual vessels. They require detailed knowledge of the vascular geometry, unlike the continuum models, which account for the blood perfusion by means of the effective conductivity of the tissue, which is dependent on the blood flow rate, or by means of other global parameters.

2.1. Continuum models

2.1.1. The Pennes equation

The first continuum model was introduced by PENNES in 1948 to analyse heat transfer in a resting human forearm [37]. The equation has the following form:

$$\rho_t c_t \frac{\partial T_t}{\partial \tau} = \lambda_t \nabla^2 T_t + w_{\mathrm{bl}} c_{\mathrm{bl}} (T_a - T_t) + q_v, \tag{1}$$

where λ is thermal conductivity [W/(mK)], ρ and c are the density [kg/m^3] and specific heat [J/(kgK)], respectively. The subscript bl labels the blood, t – the tissue, q_v is the volumetric, metabolic heat generation rate [W/m^3]; T_a denotes the arterial supply blood temperature and w_{bl} is the blood perfusion rate. When modelling hyperthermia treatment with volumetric energy deposition the right-hand side of equation (1) needs to be supplemented with an appropriate term. The internal heat generation rate is, in general, dependent on temperature. Studies of metabolism of fevered patients indicate that whole-body heat generation increases by some 0.7% for each 0.5 °C increase in temperature, giving an approximate relation, cf. [31]

$$Q_v = 85 \cdot 1.07^{T-310/0.5} \text{ [W]}. \tag{2}$$

In this equation, we have adopted a useful convention of using lower-case letters for intensive quantities and upper-case – for extensive ones. Hence Q_v denotes the overall heat generation rate (per whole body), while q_v – its density, as used in equation (1).

Table 1. Blood perfusion rates of various human tissues in [cm^3/(100g min)], after [19]

Tissue	Normal perfusion	Maximum perfusion
Skeletal muscle	2.5	60
Liver	29	176
Heart	70	400
Fat	8	30
Skin	200	497
Kidney	400	466

Basically, the Pennes equation (1) is the classical equation of heat transport supplemented with a linear heat sink, which arises from the thermal equilibration of the

blood in capillaries with the surrounding tissue. The idea behind the Pennes equation is that the blood is supplied to the tissue at an arterial temperature T_a, perfuses the tissue at the rate w_{bl} [kg/(m^{3}s)], attaining the thermal equilibrium with it and then is collected in the veins. The perfusion rate is thus the key parameter in calculating the heat transfer. Blood perfusion rates in different tissues are estimated in table 1. The data provided by Valvano (1987) are cited by DAVIDSON et al. in [19].

As shown in table 1, the values of maximum perfusion rate are often greater by an order of magnitude than those encountered in regular conditions. An increase in the perfusion rate value can occur as a result of vasodilation, which is a temperature-dependent thermoregulatory mechanism, ([3], [50]) or can be induced pharmacologically. The effects of vasodilation, which can be modelled via the single parameter w_{bl} in the Pennes model, have been more thoroughly examined by means of vascular models, cf. [47], [48], [60] and also Section 2.2. In the hyperthermic treatment of tumors, the significant nonuniformity of the perfusion throughout the cancerous tissue has to be accounted for in order to obtain the agreement with experimental data. The necrotic core of the tumor is perfused much less than the outer boundary, where the tumor is growing. Furthermore, the geometry of the vasculature in the tumor can change rather rapidly, cf. [16]. Modelling of such nonuniformities can be done with several regions of uniform perfusion ([16], [43]) or by means of continuous function of depth, for example, for lymphosarcoma, cf. [28]

$$w_{bl} = 120 + 1513\xi^2 \ [\text{cm}^3/(100\ \text{g min})], \tag{3}$$

where $\xi = r/R$, r is the radial position within the tumor and R is the tumor radius. The formulation, analytical solution and numerical evaluation of the solution for the multi-region transient Pennes equation applicable to the cases of simple spatial variation of perfusion rate are given in [22], [23].

Pennes equation (1), also called *the bioheat equation* or *heat-sink model*, is widely used for prediction of temperature elevation during hyperthermia (cf. [16], [28], [34], [35], [42], [43]) as well as for predicting a temperature response in cryosurgical protocols (cf. [27], [40], [41]). In the latter case, the blood perfusion term is often assumed to be nonlinear with respect to temperature to account for the fact that blood flow ceases at a certain low temperature. Common usage of the Pennes model is not always accompanied by careful examination of its limits of applicability. These limitations originate from neglecting the effects of thermally significant large vessels, cf. [7]. The discussion of the shortcomings of equation (1) was conducted by numerous authors (cf. [2], [7], [8], [16], [17], [30], [53], [58], [59]) and ranged from putting emphasis on the applicability limitations [16] to complete negation of its validity [58]. The main drawbacks of the Pennes model have been outlined by WULFF [59]. Most important points are:

(i) The Pennes model assumes that blood arrives at each point in the tissue at one temperature T_a regardless of the distance, which separates that point from the supplying vessel. No transport mechanism has been found to accomplish such a requirement.

Furthermore, the local arterial temperature depends on the temperature gradient in the tissue resulting from environmental conditions as shown in [8].

(ii) The blood perfusion term fails to account for the directed character of the blood flow.

(iii) The blood perfusion term has been obtained via the *global* energy balance for blood and is applied to describe *local* energy balance for tissue.

(iv) The first-order differentiability condition of numerous physical entities in the equations like heat flux, physical properties and heat generation is not necessarily met in heterogeneous tissue structures.

The Pennes equation is also unable to account for local temperature variations caused by large vessels, a feature inherent to all continuum models and unacceptable in certain applications like localised hyperthermia. The tumor regrowth that is usually reported to occur in the immediate vicinity of blood vessels most probably results from underheating of these locations. This is caused by intense cooling by blood, cf. [8].

The tissue temperature in the Pennes model is typically defined, cf. [2], [11]

$$T_t(\mathbf{x}) = \frac{1}{V}\int_V T(\mathbf{x})\,dV, \tag{4}$$

where the scale of the averaging volume V is assumed to be much larger than the size of thermally significant vessels and much smaller than the size of the tissue region itself. BAISH [2] has pointed out that no such scale exists because the vascular tree consists of vessels of virtually all sizes.

Table 2. Properties of different kinds of blood vessels after [11]

Vessel	Percentage of vascular volume	Avg. radius [μm]	Avg. length [mm]	x_{eq} [mm]
Aorta	3.30	5000	380	190000
Large artery	6.59	1500	200	4000
Arterial branch	5.49	500	90	300
Terminal arterial branch	0.55	300	8	80
Arteriole	2.75	10	2	0.005
Capillary	6.59	4	1.2	0.0002
Venula	12.09	15	1.6	0.002
Terminal vein	3.30	750	10	100
Venous branch	29.67	1200	90	300
Large vein	24.18	3000	200	5000
Vena cava	5.49	6250	380	190000

x_{eq} – thermal equilibration length.

The thermal equilibration length in the Pennes model is assumed to be infinite for all vessels except the capillaries and zero for capillaries. This is also a nonphysical assumption. In table 2, the estimates of this value are given for different kinds of vessels, see also figure 2 [3], [4], [53]. We recall that the thermal equilibration length has

been defined by CHEN and HOLMES [11] as the length over which the temperature difference between the tissue and the blood is reduced by the factor *e*.

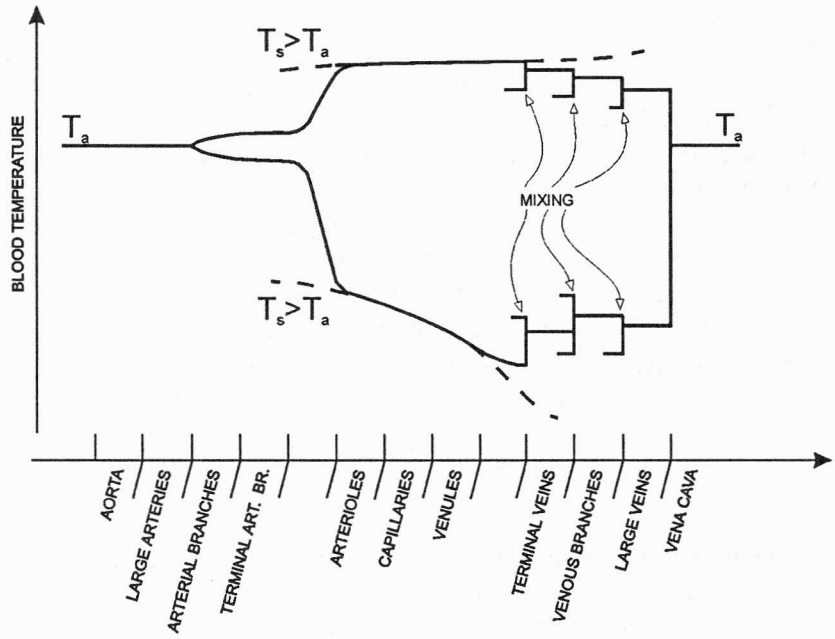

Fig. 2. Temperature of blood as it circulates through the vascular system, after [11]

The Pennes equation can be supplemented with the correction factor – the efficiency coefficient, multiplying the heat-sink term in equation (1). It accounts for the thermal equilibration of the returning vein (thus making allowance for the fact that the returning venous blood temperature may differ from tissue temperature). This coefficient is a function of the complex geometry of the system and its derivation is described in detail in [55].

In spite of the serious criticism of the Pennes model, its predictions are often superior to those of more elaborate formulations (see the effective conductivity models below). This fact gives rise to the need for reconsidering the physical foundations of the approach. CHARNY et al. [9] have suggested that the blood perfusion term in equation (1) does not represent the isotropic thermal equilibration in capillaries, but describes the small vessel bleed-off occurring in the regions of the largest countercurrent vessels and supplying the capillary bed in tissue. In this manner, the temperature of the blood entering these capillaries is the temperature of the blood in the largest vessels. In the region dominated by smaller vessels, this condition is not always satisfied and models other than equation (1) are preferred [9].

An issue that is important in assessing the predictive capabilities of any model is the uncertainty originating from the fact that only approximate values of model pa-

rameters are usually known. This is even more pronounced in the field of biomechanics, where the scatter of measurements is always considerable. Typical values of the Pennes model parameters are presented in table 1 and table 3. In [33], the analysis of the uncertainty arising from the approximate character of the model parameters in the Pennes equation applied to the typical hyperthermia treatment was performed. The analysis assumed power deposition by laser or microwave governed by Beer's law:

$$q_r(x) = \eta P_0 e^{-\eta(L-x)}.$$

The variable x denotes the depth in the tissue, L is the position of the skin surface.

Table 3. Values of thermal properties of tissue used in several applications of models of bioheat transfer

Model	Tissue specific heat c_t [J/(kgK)]	Blood specific heat c_{bl} [J/(kgK)]	Tissue thermal conductivity λ_t [W/(mK)]	Metabolic heat generation rate q_m[W/m^3]
Jiji et al., 3-layer vascular model [29]	steady-state model	3800	0.5	0
Durkee et al., numerical evaluation of Pennes equation [23]	3800	3300	1.6	145
Brinck and Werner, 3D vascular model [8]	3800	3800	0.465	245 – extremity at rest and core and fat layer in exercise conditions 24500 – muscle layer in exercise conditions
Shitzer et al., numerical model of extremity [46]	2102 – extremity core 3136 – muscle 2520 – fat 3780 – skin	3899	1.064 – extremity core 0.418 – muscle 0.204 – fat 0.293 – skin	170.5 – extremity core 631.9 – muscle 5.0 – fat 247.4 – skin (basal values)
Song et al., combined macro- and microvascular limb model [49]	steady-state model	3800	0.5 – intrinsic conductivity (non-perfused tissue), effective value predicted by model	Dependent on model parameters and blood inflow Peclet number: 245 – for supine resting state 2430 – for moderate exercise

The parameters under consideration were the thermal conductivity λ, the blood perfusion rate w_{bl}, metabolic heating rate q_m, the scattering coefficient η and the applied power P_0. The volumetric heat generation rate is expressed as:

$$q_v = q_m + q_r .$$

The measure of temperature uncertainty ΔT is defined:

$$\Delta T = \sqrt{\left(\frac{\partial T}{\partial \lambda}\Delta\lambda\right)^2 + \left(\frac{\partial T}{\partial w_{\mathrm{bl}}}\Delta w_{\mathrm{bl}}\right)^2 + \left(\frac{\partial T}{\partial q_m}\Delta q_m\right)^2 + \left(\frac{\partial T}{\partial \eta}\Delta\eta\right)^2 + \left(\frac{\partial T}{\partial P_0}\Delta P_0\right)^2} .$$

It can be expressed in terms of the relative uncertainties as follows:

$$\frac{\Delta T}{T} = \sqrt{\left(\frac{\partial \ln T}{\partial \ln \lambda}\frac{\Delta\lambda}{\lambda}\right)^2 + \left(\frac{\partial \ln T}{\partial \ln w_{\mathrm{bl}}}\frac{\Delta w_{\mathrm{bl}}}{w_{\mathrm{bl}}}\right)^2 + \left(\frac{\partial \ln T}{\partial \ln q_m}\frac{\Delta q_m}{q_m}\right)^2 + \left(\frac{\partial \ln T}{\partial \ln \eta}\frac{\Delta\eta}{\eta}\right)^2 + \left(\frac{\partial \ln T}{\partial \ln P_0}\frac{\Delta P_0}{P_0}\right)^2} .$$

In figure 3, the various contributions to overall uncertainty are presented against the temperature profile during the simulated 1-D surface heating of the specimen [33]. The greatest contributions come from the blood perfusion rate, the power flux applied and the conductivity uncertainties. The influences of metabolic rate and scattering coefficient are negligible which means that the accurate determination of these parameters is altogether not critical for the accurate determination of the temperature field. The effect of metabolic heat generation is in fact omitted by many researchers working on hyperthermia.

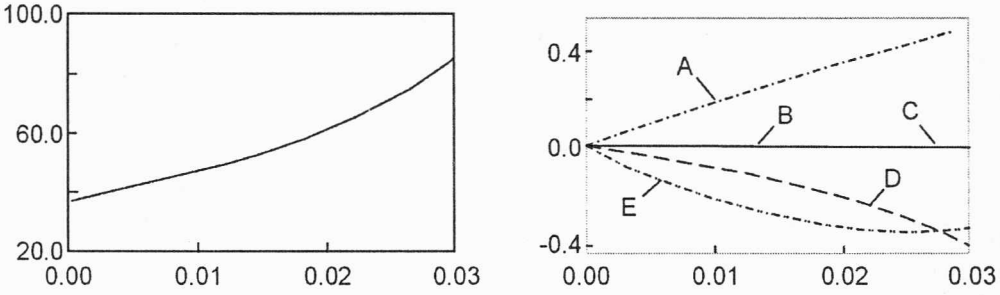

Fig. 3. Temperature distribution (°C) calculated in accordance with the Pennes model (1) and the sensitivities, as a function of spatial coordinate.
A: $\frac{\partial \ln T}{\partial \ln P_0}$, B: $\frac{\partial \ln T}{\partial \ln \eta}$, C: $\frac{\partial \ln T}{\partial \ln Q_m}$, D: $\frac{\partial \ln T}{\partial \ln \lambda}$, E: $\frac{\partial \ln T}{\partial \ln w_b}$, after [33]

Similar investigations of parameter sensitivity in the Pennes equation have been conducted by MAJCHRZAK and JASIŃSKI, [34] for the 2-D transient temperature field in the cutaneous region of the tissue subjected to external heat source. These authors examined the sensitivity to specific heat, tissue thermal conductivity and the blood perfusion rate. Their results indicate significant temperature field sensitivity to thermal conductivity and negligible sensitivity to other parameters considered. This is inconsistent with findings of LIU [33] who has found sensitivity to blood perfusion rate to have a profound contribution, see figure 3. The reason for this may be the fact that this author considered a significantly lower base value of the blood perfusion –

2000 [W/(m^{3}K)] compared to 5000 [W/(m^{3}K)] used in [34]. LIU [33] also expressed his results in terms of relative uncertainties: $\partial \ln T/\partial \ln \lambda$ instead of plain $\partial T/\partial \lambda$ as in [34] which might have biased the interpretation.

2.1.2. Directed perfusion model

The second continuum model is the directed perfusion model proposed by WULFF in 1974 [58]. Its derivation relies on the assumption that, unlike in the Pennes model, the blood is completely equilibrated with the tissue all the time. Recall that in the heat-sink model it is assumed to retain *arterial temperature* until it reaches the capillaries and then to momentarily equilibrate with tissue. When the energy transport is assumed to be not only due to the conduction but also due to the convection by the moving blood (in equilibrium with the tissue) the energy flux according to WULFF [58] is as follows:

$$\mathbf{q} = -\boldsymbol{\lambda}_t \nabla T_t + \rho_{\mathrm{bl}} h_{\mathrm{bl}} \mathbf{U}, \tag{5}$$

where h_{bl} is the specific blood enthalpy and $\mathbf{U}$ is the Darcy velocity of the blood flow. The first term on the r.h.s. in equation (5) is the usual Fourier-law conductive flux. The second term accounts for the blood directed convection.

Inserting equation (5) into the energy balance equation and putting $T_{\mathrm{bl}} = T_t$ one arrives at

$$\rho_t c_t \frac{\partial T_t}{\partial \tau} = \lambda_t \nabla^2 T_t - \rho_{\mathrm{bl}} c_{\mathrm{bl}} \mathbf{U} \cdot \nabla T_t + q_v. \tag{6}$$

It should be noted that this model applies to cases where the blood is in equilibrium (or in quasi-equilibrium) with the tissue and during hyperthermic treatments it is often not the case (cooling effect of the large vessels is then pronounced). A quick glance at figure 2 and the data in table 2 indicate that the assumptions leading to equation (6) are valid only in a certain range of physical situations strongly dependent on the kind of vasculature. CREEZE and LAGENDIJK [17] have also pointed out that the blood flow is not always unidirectional, vessels are often combined to form countercurrent pairs and their orientation is frequently isotropic.

2.1.3. Effective conductivity models

The *effective conductivity* models (also termed k_{eff} or λ_{eff} models) treat the energy transport in the tissue in terms of heat conduction only. The effect of vascularity is contained in the thermal conductivity term which is often assumed to be isotropic and dependent on the blood perfusion w_b. The dependence usually assumed is of the form

$$\lambda_{\mathrm{eff}} = \lambda_t (1 + \alpha_1 w_{\mathrm{bl}})$$

or

$$\lambda_{\text{eff}} = \lambda_t (1 + \alpha_2 w_{\text{bl}}^2),$$

where λ_t is the intrinsic thermal conductivity of the tissue and α_1, α_2 are the parameters that depend on the vessel size and density.

Theoretical foundations of the effective conductivity model have been laid down by WEINBAUM and JIJI [52]. On the basis of the knowledge of anatomical structure of vasculature and with the aid of several simplifying assumptions they developed a compact formulation of the heat transfer equation in the soft tissue. The authors called their model the *simplified bioheat equation* because it is a simplified form of some of the ideas derived from vascular models that are described in Section 2.2. The Weinbaum–Jiji effective conductivity model is derived with the following crucial assumptions [52]:

- the energy equation is formulated in terms of a single local average blood–tissue temperature,
- local average blood temperature can be approximated by the local tissue temperature,
- the primary heat transfer mechanism is the incomplete countercurrent exchange in thermally significant vessels (greater than 40 μm in diameter), which means that the heat loss from the artery is *nearly but not quite* equal to the heat gained by the vein.

Using these assumptions and considering the closely spaced, countercurrent artery–vein pairs Weinbaum and Jiji derived the expression for the effective conductivity tensor [52]:

$$\lambda_{ij}^{\text{eff}} = \lambda_t \left(\delta_{ij} + \frac{n\pi^2 r^2}{4\sigma} \left(\frac{\lambda_{\text{bl}}}{\lambda_t} \right) Pe^2 l_i l_j \right), \tag{7}$$

where n is the vessel number density (geometrical parameter of the vasculature), r is the vessel radius (assumed equal for artery and vein), l_i are the direction cosines of the vessels relative to the coordinate axes and $\boldsymbol{\delta} = (\delta_{ij})$ is the Kronecker delta. Pe is the blood flow Peclet number defined by

$$Pe = Pr\, Re = \frac{2\rho_{\text{bl}} c_{\text{bl}} r u}{\lambda_{\text{bl}}}, \tag{8}$$

where Pr and Re are Prandtl and Reynolds numbers, respectively, and u is the average blood flow velocity. Moreover, σ is the shape coefficient describing the thermal coupling between the countercurrent artery and vein obtained from the consideration of two-dimensional conduction in the plane perpendicular to the axes of vessels.

We have

$$\sigma = \frac{\pi}{\cosh^{-1} \dfrac{l(S)}{2r(S)}}, \tag{9}$$

where l is the distance between the axes of the countercurrent vessels at the point determined by the coordinate S along the axis of the vessels.

From (7) we infer that the effective conductivity derived by WEINBAUM and JIJI [52] is the tissue intrinsic conductivity with an additional term accounting for the countercurrent convection.

The Weinbaum–Jiji effective conductivity model energy equation is derived [52] in the form:

$$\rho c \frac{\partial T}{\partial \tau} = \frac{\partial}{\partial x_i}\left(\lambda_{ij}^{\text{eff}} \frac{\partial T}{\partial x_j}\right) + q_v - \frac{\pi^2 n r^2 \lambda_{2\text{bl}}^2}{4\sigma\lambda_t} Pe^2 l_j \frac{\partial l_i}{\partial x_i}\frac{\partial T}{\partial x_j}. \tag{10}$$

This equation is the ordinary Fourier–Kirchhoff equation for the heat conduction in anisotropic media with an effective conductivity and an additional term on the r.h.s. This term accounts for the possible variation of vessel radius along its length and for the directed capillary perfusion between artery and vein. It is small and vanishes entirely when the vessels are straight. Obviously, the summation convention over the repeated indices applies to the equation (10).

From equation (7) the formula for the effective scalar conductivity in one-dimensional case can be obtained:

$$\lambda^{\text{eff}} = \lambda_t\left(1 + \frac{n\pi^2 r^2}{4\sigma}\left(\frac{\lambda_{\text{bl}}}{\lambda_t}\right)Pe^2\right). \tag{11}$$

As estimations by Weinbaum and Jiji indicate, for a tissue with vessels that have the radius of more than 100 μm, the enhancement in conductivity is noticeable and for larger vessels the effective conductivity is several times larger than the tissue intrinsic property.

The above-mentioned assumptions leading to the development of the Weinbaum–Jiji bioheat equation, mainly that the average arterio-venous temperature is equal to tissue temperature, have been criticized in [8] and [56]. Results of computations on elaborate vascular model by Brinck and Werner contradict this assumption, cf. [8].

The existence and importance of countercurrent heat exchange at the certain vessel scale range have been confirmed by numerous experiments both in normothermic (i.e. when tissue is at physiological temperature) and hyperthermic (vasodilated) states, cf. [47], [48], [60], [61].

The effective conductivity models do not depend explicitly on arterial temperature. Increase of the blood flow rate results therefore in enhancement of the effective conductivity of the tissue, regardless of whether warm blood perfuses cold tissue or cold blood perfuses warm tissue. Consequently, perfusing a cooler tissue with warm blood will result in the decrease in temperature owing to enhanced conduction to the surface – the effect opposite to that predicted by Pennes equation (1). WISSLER [56] argues that this discrepancy is in favour of the latter and proposes supplementing the Pennes equation with additional "efficiency factor" to account for the incomplete countercurrent heat exchange in a simple way.

WEINBAUM and JIJI [54] have suggested that a hybrid model, consisting of the Pennes model and the effective conductivity approach, should be used. They propose that the thermal equilibration parameter (thermal equilibration distance normalized by the length of the representative vessel):

$$e = \frac{\pi r Pe}{2\sigma L} \tag{12}$$

should be used to distinguish whether the Pennes model ($e > 0.3$) or the Weinbaum–Jiji bioheat equation ($e \leq 0.3$) applies. Similar suggestions were made by CHARNY et al. [9], who compared the normothermic and hyperthermic responses of the Weinbaum–Jiji λ_{eff} model, the Pennes model and more sophisticated three-equation model. The main conclusion of their study is that the Pennes model provides a relatively good prediction capabilities and should be therefore incorporated in the proposed hybrid model by means of criterion (12). This means that under normothermic conditions equation (1) should be used in the regions of tissue containing the first generations of supply vessels (larger than 500 μm in diameter). As the study by CHARNY et al. [9] have shown, neglecting the countercurrent heat exchange in these regions does not lead to any serious discrepancies. The Weinbaum-Jiji model is more suitable in the regions of tissue containing smaller vessels.

Limitations of applicability of the Weinbaum–Jiji bioheat equation were also confirmed by VALVANO et al. [51] by means of analysis and thermistor measurement of temperature field in the canine cortex.

The validity of effective conductivity approach was tested by BAISH [1], who viewed the tissue with embedded countercurrent vessels as a composite material consisting of low-conductivity tissue matrix and high-conductivity fibers representing paired countercurrent vessels. This author obtained the following formula for the fiber conductivity:

$$\lambda_f = \frac{(\dot{m} c_{\text{bl}})^2}{2lr\pi^2\lambda} \cosh^{-1}\left(\frac{l}{r}\right), \tag{13}$$

where $2l$ is the distance between axes of the countercurrent vessels.

Because of the quadratic dependence on the blood flow rate, the conductivity computed using equation (13) varies in a very wide range. For example, for the vessels that have the radius of 300 μm the respective fiber conductivity exceeds 3000 [W/mK], and for the vessel radius of 500 μm this conductivity is 320 000 [W/mK]. No real material has such a high conductivity. This result is explained by the fact that the convection, really taking place within the veins, is much more efficient heat transfer mechanism than the conduction. The intrinsic conductivity of the tissue is of the order of 0.2–0.6 [W/mK] and the fibrous composites containing fibers that are much more conductive than the matrix are known to be poorly modelled by the effective conductivity, cf. [1]. If we consider the array of parallel countercurrent vessel pairs

embedded in the tissue lying along the z-axis and impose an external temperature gradient parallel to the axes of vessels, the total heat flux can be expressed by [1]:

$$q = -\lambda_t \frac{\partial T_t}{\partial z} + n(q_{\text{artery}} + q_{\text{vein}}),$$

where $(q_{\text{artery}} + q_{\text{vein}})$ is the heat exchange with tissue by single vessel pair. So, the effective conductivity approach is admissible only if $(Q_a + Q_v)$ is proportional to the tissue temperature gradient dT_t/dz. Heat exchange by blood vessel pair is, however, proportional to the gradient of mean blood temperature T_m. Therefore, the assumption by Weinbaum and Jiji that $dT_t/dz = dT_m/\text{dz}$ is necessary in the derivation of effective conductivity model, cf. [1].

The three continuum models of heat exchange in perfused tissues described above can be used to construct a mixed model. For example, CHEN and HOLMES [11] suggest that thermal contributions from individual large vessels should be calculated separately and for the bio-heat equation they propose the following formulation:

$$\rho_t c_t \frac{\partial T_t}{\partial \tau} = \nabla \cdot (\lambda^{\text{eff}} \nabla T_t) + w^*_{\text{bl}} c_{\text{bl}} (T^*_a - T_t) - \rho_{\text{bl}} c_{bl} \mathbf{U} \cdot \nabla T_t + q_v, \tag{14}$$

where w^*_{bl} and T^*_a are the perfusion rate and arterial temperature, respectively, modified to avoid double-counting of the contribution of large vessels.

CREZEE et al. [18] considered a mixed heat sink – effective conductivity approach formulated in the following equation:

$$\rho_t c_t \frac{\partial T_t}{\partial \tau} = \lambda^{\text{eff}} \nabla^2 T_t + f w_{\text{bl}} c_{\text{bl}} (T_a - T_t) + q_v, \tag{15}$$

where f is a model parameter dependent on the local vascularity structure. It can be shown that for closed vessel network $0 \leq f \leq 1$.

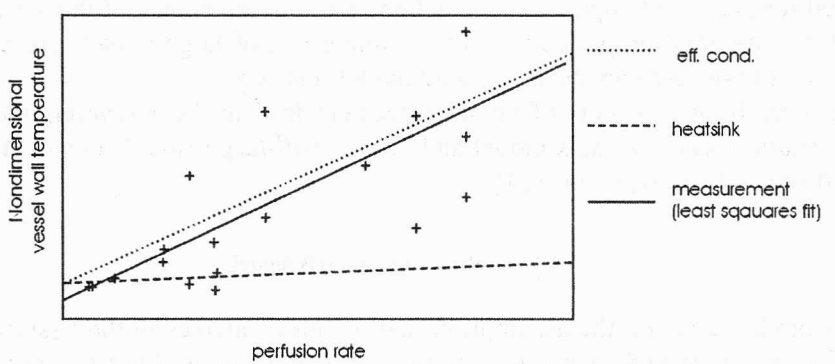

Fig. 4. Comparison of the effective conductivity and the Pennes (heatsink) model predictions with measurements; "+" denotes a measurement data point, after [17]

The experimental verification of the continuum models presented was performed in [17] and [18]. In [17], the measurements of temperature field in bovine kidney cortex were conducted. The comparison between the heat-sink and the effective conductivity models were generally in favour of the λ_{eff} theory although the scatter of the measurements was considerable, as can be seen in figure 4. In this figure, the non-dimensional temperature of the vessel wall is depicted against perfusion rate ranging from 0 to 55 cm^3/(100 g min). The non-dimensional temperature is defined:

$$\theta = \frac{T - T(R)}{T(0) - T(R)},$$

where $T(0)$ denotes the temperature at the centre of the tissue cylinder considered and $T(R)$ – at its outer boundary. In figure 4, θ ranges from 0 to 9.

Other results indicate that the increase of the perfusion from 0 to 38 cm^3/(100 g min) caused a significant decrease of the vessel wall temperature suggesting a 6-fold decrease in the thermal resistance of perfused tissue. The prediction of the Pennes model yields a 15% decrease. Other tests confirmed that the λ_{eff} model is superior to the heat-sink model, especially in small-scale predictions. In the case of larger vessels, the use of discrete (vascular) description is preferred [18].

ROEMER and DUTTON [44] argued that the Pennes perfusion term and the effective conductivity are nonphysiological quantities that are related to the true capillary perfusion in a problem-dependent manner. They provide detailed derivation of the universal tissue convective energy balance equation.

2.2. Vascular models

The idea behind developing vascular heat transfer models for soft tissues is to use the data of actual placement of blood vessels within the tissue to predict the heat flow. The need for accurate temperature predictions arose in the course of the development of modern hyperthermic protocols. The cooling effect of large vessels present at the site of target tissue escapes the continuum models entirely.

The three basic concepts of vessel placement lead to the *unidirectional vessels* model, *countercurrent vessels* model and *large-small-large vessels* model. These are briefly discussed below, cf. also [3].

2.2.1. Unidirectional vessels model

This model relies on the assumption that the blood arrives in the tissue at artery supply temperature and exchanges its heat with the tissue along the vessel. Two unknown quantities, namely: the tissue temperature T_t and the vessel blood temperature T_{bl} are considered. Both are defined along the vessel as the local average quantities:

$$T_t(S) = \frac{1}{A_t} \int_{A_t} T d\, A, \tag{16}$$

$$T_{\mathrm{bl}}(S) = \frac{1}{A_{\mathrm{bl}}} \int_{A_{bl}} T d\, A, \tag{17}$$

where A_t and A_{bl} are domains occupied by the tissue and the blood depicted in figure 5 as the grey ring and white circle, respectively. The energy conservation in a tissue cylinder surrounding blood vessel is considered.

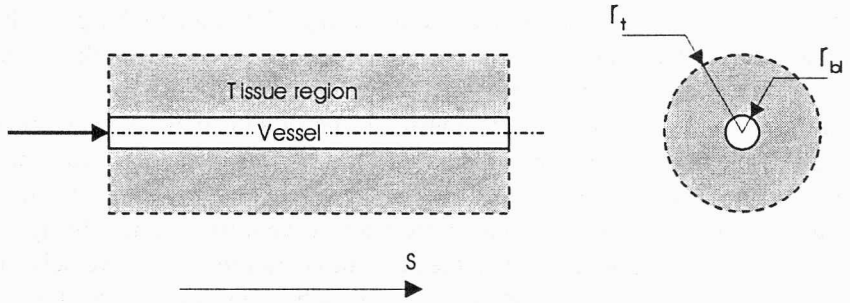

Fig. 5. Generic tissue cylinder considered in the model of unidirectional vessels

The equation for the tissue is [3], [4],

$$\rho_t c_t \frac{\partial T_t}{\partial \tau} = \lambda \frac{\partial^2 T_t}{\partial S^2} - n q_{\mathrm{bl}} + q_v, \tag{18}$$

where n is the vessel density and q_{bl} is the rate of heat flow into the vessel in [W/m] derived from the energy balance for vessel:

$$q_{\mathrm{bl}} = \pi r_{\mathrm{bl}}^2 \rho_{\mathrm{bl}} c_{\mathrm{bl}} \overline{u} \frac{dT_{\mathrm{bl}}}{dS}. \tag{19}$$

Here $\overline{u}$ is the bulk blood velocity in the vessel and S is the distance measured along the vessel, whether it be straight or curved. Let us introduce the convection boundary condition on the vessel wall:

$$q_{\mathrm{bl}} = 2\pi r_{\mathrm{bl}} \alpha (T_w - T_{\mathrm{bl}}), \tag{20}$$

where α is the convection film coefficient [W/(m^{2}K)] and T_w is the vessel wall temperature. If q_{bl} is phrased in terms of the temperature difference $(T_t - T_a)$:

$$q_{\mathrm{bl}} = \lambda_t \sigma_a (T_t - T_{\mathrm{bl}}), \tag{21}$$

then the shape coefficient can be obtained from the consideration of the heat transfer in the plane perpendicular to the vessel axis [4]:

$$\sigma_a = \frac{2\pi}{\ln \frac{r_t}{r_{bl}} + \frac{\lambda_t}{\lambda_{bl}} \frac{2}{Nu} - \frac{1}{2}}, \tag{22}$$

where Nu is the Nusselt number of the flow inside the vessel:

$$Nu = \frac{\alpha l_0}{\lambda_{bl}}. \tag{23}$$

According to CHATO [10] Nu is equal to 4, cf. also [4]; l_0 is the characteristic dimension of the flow equal to the vessel diameter $2r_0$. The value of Nu given here corresponds to vessels large enough, whose diameters are much larger than size of the blood cells. This is not the case of the microcirculation, [36].

Equation (18), (19), (21) and (22) constitute the unidirectional vessels model. The model neglects the heat conduction in the blood along the vessel and the heat generation in the blood. Furthermore, as experimental tests of the vasculature indicate, all major vessels start out as a closely juxtaposed countercurrent artery–vein pairs. They diverge substantially forming a roughly periodic array in the generation prior to terminal vessels, cf. [53].

The heat conduction shape coefficient approach, consisting in relating the heat transfer to vessels to the blood–tissue temperature difference by means of the proportionality coefficient obtained from planar steady-state analysis, is successfully used in other formulations presented below.

2.2.2. Countercurrent vessel model

In this formulation, the vessels are assumed to exist only in the form of countercurrent artery–vessel pairs distributed with the density n. In this model, the basic mechanisms of heat transfer are countercurrent heat exchange between arteries and veins and the vessel–tissue heat transfer. The difference between arterial and venous blood temperature is considered to be the driving force of the former, while the difference between *average* temperature in both vessels and the tissue is assumed to cause the latter mode of heat exchange. Note that for two vessels located symmetrically in the tissue cylinder (see figure 6), close to each other, the difference in temperature between the vessels does not influence the net heat transfer to the tissue [4]. In the previously described models, countercurrent exchange was not present.

The model considered contains three key variables: the tissue, artery blood and vein blood temperatures, denoted by T_t, T_a and T_v, respectively. The equations are constructed using the shape coefficient formalism, cf. [3], [4]. Finally we get:

(i) in the tissue

$$\rho_t c_t \frac{\partial T_t}{\partial \tau} = \lambda_t \frac{\partial^2 T_t}{\partial S^2} - n\lambda_t \sigma_\Sigma \left(T_t - \frac{T_a + T_v}{2} \right) + q_v, \tag{24}$$

(ii) in the artery (feeding vessel)

$$\pi r_0^2 \rho_{bl} c_{bl} \overline{u} \frac{\partial T_a}{\partial S} = \lambda_t \sigma_\Delta (T_v - T_a) + \frac{\lambda_t \sigma_\Sigma}{2} \left(T_t - \frac{T_a + T_v}{2} \right), \tag{25}$$

(iii) in the vein (draining vessel)

$$\pi r_0^2 \rho_{bl} c_{bl} \overline{u} \frac{\partial T_v}{\partial S} = \lambda_t \sigma_\Delta (T_v - T_a) - \frac{\lambda_t \sigma_\Sigma}{2} \left(T_t - \frac{T_a + T_v}{2} \right). \tag{26}$$

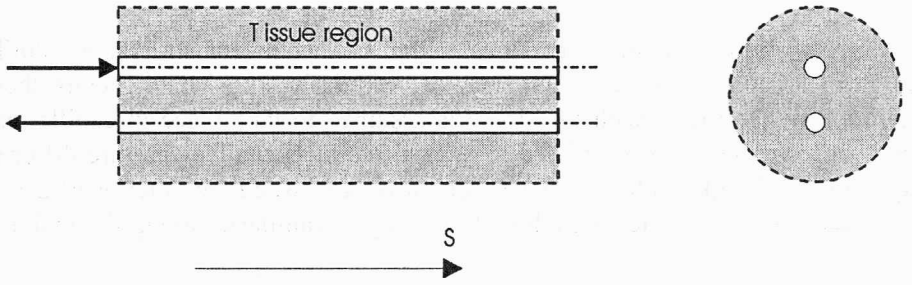

Fig. 6. Generic tissue cylinder considered in the model of countercurrent flow vessels

Here σ_Δ is the shape coefficient for the heat exchange between individual vessels in the countercurrent pair, while σ_Σ is the shape coefficient for the heat exchange between vessel pair and tissue. These coefficients are estimated, similarly as in the model of unidirectional vessels, on the basis of considerations of steady-state temperature distributions in the plane normal to the axes of the vessels, using the superposition method. The derivation, along with values for several kinds of vessels, is given in [4].

2.2.3. Large–small–large model

This model is somewhat simplified in comparison with the last one. It relies on the assumption that vasculature has a hierarchical structure with large arteries feeding smaller and smaller vessels, which in turn feed the capillaries, see figure 7. The blood from capillaries drains into larger and larger vessels, which eventually feed the large veins that are countercurrent with the large arteries. The most important assumption here is that significant heat transfer with the tissue occurs only at the level of capillaries. The thermal coupling between the large vessels and the tissue σ_Σ in equations (25), (26) is assumed to be small and the equilibration length in the capillaries to be much shorter than their length. This common belief is in contradiction to findings of CHEN and HOLMES [11], see also table 2, figure 2 and the discussion below.

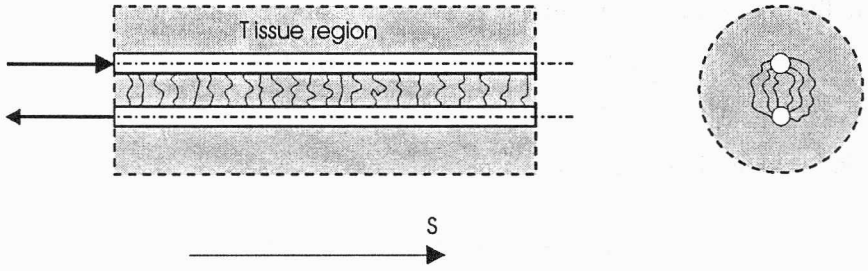

Fig. 7. Generic tissue cylinder considered in the model of large–small–large vessels

In this model, the heat-sink term is employed to account for vasculature similarly to the Pennes model (1), see Section 2.1.1. Similarly, the instantaneous thermal equilibration of the blood with the tissue is assumed to take place in capillaries, so this heat-sink strength is proportional to arterial blood–tissue temperature difference, see equation (1). Unlike in the Pennes model, it is expressed here in terms of decay of the blood flow in artery due to the blood draining to capillaries along the major vessel:

$$\rho_t c_t \frac{\partial T_t}{\partial \tau} = \lambda_t \frac{\partial^2 T_t}{\partial S^2} + \rho_{\mathrm{bl}} c_{\mathrm{bl}} \left(T_t - T_a\right) \frac{\partial}{\partial S}\left(n\pi r_0^2 \overline{u}\right) + q_v . \tag{27}$$

The last equation reduces to the Pennes equation (1) provided that

$$w_{\mathrm{bl}} = -\rho_{\mathrm{bl}} \frac{\partial}{\partial S}\left(n\pi r_0^2 \overline{u}\right). \tag{28}$$

The model presented and the Pennes model are conceptually different. Equation (28) should be understood as a certain idealisation applied at a scale that is not too small. Otherwise, when individual capillary branches are considered, the flow along the major vessel becomes discontinuous and therefore equation (28) becomes useless.

BAISH et al. [3] made a comparison of the above-mentioned vascular and continuum models. These authors concluded that in limiting cases, with respect to the vessel thermal equilibration length, the predictions of vascular models approached the predictions of continuum models.

The linear heat-sink behaviour, such as that found in the Pennes equation, exists only in the large–small–large vascular model. This model, however, implies the existence of large vessels that are not equilibrated with the tissue and which are the source of the local temperature nonuniformities that escape the Pennes model completely. The magnitude of these nonuniformities can be comparable to the predicted temperature elevation due to the heat source, see also [58].

The vascular heat transfer models presented above are meant to be used in the case of complex geometry of the vascular system. This is a formidable task and identification of thermally significant vessels, in order to simplify it, is fully justified. Since the main drawback of the continuum models is that they cannot predict local temperature

irregularities caused by the presence of large, relatively sparsely distributed vessels, which are easy to identify, it is reasonable to construct mixed models. Such models account for each large vessel individually and all "small" vessels are modelled via the heat-sink type term or via the effective conductivity. The important question is which vessels are small enough.

In figure 2, the possible temperature of blood element as it passes through the vascular system is depicted. The two dashed lines denote the temperatures of the two kinds of the solid tissue that the blood element can encounter during its transport – namely cooler and warmer than T_a (arterial temperature). As investigations of CHEN and HOLMES [11] indicate and as can be inferred from figure 2, the equilibration of the blood with the solid tissue takes place between the terminal arterial branches and the precapillary arterioles, not in the capillaries as it was usually previously assumed.

This hypothesis was fully supported by the experimental investigations due to LEMONS et al. [32] and WEINBAUM et al. [53] who measured the temperature field in the rabbit thigh *in vivo* in order to identify the thermally significant vessels. Their measurements indicate that all arteries of the diameter $d_a < 100$ μm and all veins with $d_v < 400$ μm can be considered fully equilibrated with the surrounding tissue in normothermic conditions. This needs not to be true during hyperthermic or cryogenic treatment.

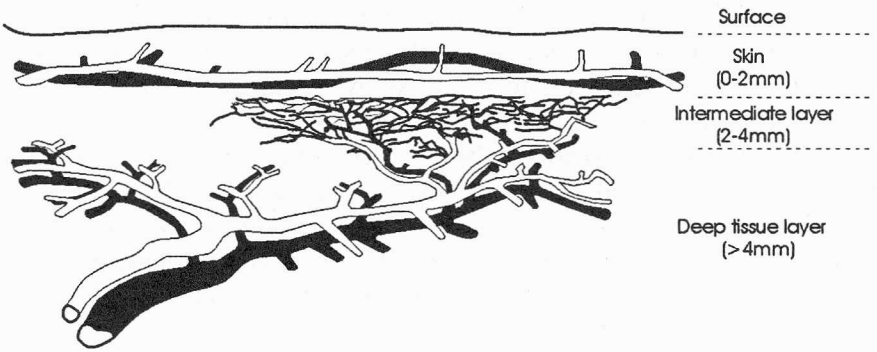

Fig. 8. Three essential layers of peripheral circulation distinguished by WEINBAUM et al. [53]

As can be seen from the above considerations, modelling techniques for large vessels and capillary vasculature are different. Following this observation and the extensive anatomical study of the surface tissue WEINBAUM et al. [53] proposed a three-layer model of microcirculation contributing to the heat transfer in soft tissue, cf. also [29]. The model contains layers depicted in figure 8:

• *Deep tissue layer.* The thick region of thermally significant large veins and arteries. For four or more generations they proceed as closely juxtaposed branching countercurrent artery–vein pairs. The cross-sectional surface areas of these vessels are large and their characteristic thermal equilibration lengths are large compared to their lengths (see table 2.). In this layer, the thermal state is characterized by three different temperatures, namely of arterial blood, of venous blood and of local tissue. The

countercurrent exchange between paired vessels is the dominant mode of the heat transfer here. These large vessels during their final generations gradually transform to a periodically arranged array of terminal vessels at the bottom of the next layer.

• *Intermediate layer.* Blood is assumed to equilibrate almost immediately with the tissue when it enters this layer. The thermal state is therefore characterized by the local tissue temperature only, so individual vessels are no longer considered. Horizontal temperature gradients may exist due to temperature nonunuformities in the preceding layer. Terminal vessels are assumed to be regularly spaced.

• *Skin.* This layer, also termed the cutaneous layer, contains large vessels that act as a volumetric heat source. They are far from the thermal equilibrium with the surrounding tissue. The dominant heat transfer mode is the conduction in the direction parallel to the surface.

This three-layer model of the surface tissue heat transfer is described at length by JIJI et al. [29] and WEINBAUM et al. [53].

Another three-dimensional, three-layer model of surface tissue heat transfer has been proposed by BRINCK and WERNER [8]. The example vascular geometry served for the numerical calculations in resting, exercise and cold states distinguished by different metabolic heating and environmental conditions. The blood temperature along the arterial and venous vessels and appropriate tissue temperature fields were calculated. These authors conclude that such vessel-by-vessel approach is limited to small volume of the tissue due to the lack of knowledge about the detailed, individual vascular geometry and the large size of resulting computational tasks.

This difficulty has been partly resolved by the model proposed by BAISH [2]. The algorithm of vascular growth has been developed to generate the detailed vascular geometry. The physiologically justified Gottlieb procedure was chosen. This procedure of growth process runs as follows, cf. [2] and the references therein:

1. Begin with a sparse tree containing only the supply vessel.
2. Assume the grid of cells.
3. Check the distance from each cell to the existing vascular tree.
4. If the cell is further than some threshold distance then a new vessel is added between the cell and the nearest point on the existing vascular tree.
5. Decrease the threshold distance, refine the cell grid and repeat the procedure starting from 3 until a desired density of the vasculature is reached.

The radius of the blood vessels can be obtained from modified Murray's law

$$r_i^n = \sum_j r_j^n , \tag{29}$$

where the index j denotes daughter vessels of the vessel i and the value of n is typically 2.7. The mass flow is usually related to the vessel radius by means of the equation:

$$\frac{\dot{m}_i}{\dot{m}_j} = \left(\frac{r_i}{r_j} \right)^n . \tag{30}$$

The above rules allow one to construct the entire vascular tree starting from a few supplying vessels. The generation encompasses all sizes of vessels so no arbitrary differentiation into "thermally significant" and "thermally insignificant" is necessary. Despite the simplicity of the generating algorithm and its numerous flaws the results resemble the real vasculature in many respects. Since they are not any real but "virtual" vasculature the statistical interpretation of the results of associated model of heat transfer has also been proposed [2].

An attempt to apply some of the above-specified ideas to the construction of the whole-limb heat transfer model was made by SONG et al. [49]. This model is conteptually based on the models being developed earlier cf. [29], [53]. It is based on the three-layer structure of the limb: core, muscle tissue and the cutaneous layer, the latter being subdivided further into the inner and outer skin regions, see figure 8. The limb model does not include bone tissue. The layers form a cylinder of variable cross-section. It is then discretized into disc-like elements. The arterial temperature supplying the limb is known, the venous return temperature is guessed at the beginning and obtained by an iterative procedure. The model parameters include the inflow blood Peclet number, the ratio of blood flow to arm to total blood supply to the limb, the ratio of blood flow to the muscle layer to blood supply to the arm and the parameters describing the heat loss to the environment (by the convection, radiation and evaporation). Complete mathematical formulation of the model is quite complex, and for the detail the reader is referred to [49].

2.3. Pulsatile blood flow effects

Any vascular model requires certain assumptions accepted for the heat exchange on the blood vessel level. The most common practice is to describe the blood flow in terms of the bulk average velocity and the heat transfer is then characterized using the Nusselt number as defined by equation (23). Such an approach was employed in the models described in sections 2.2.1–2.2.3. The Nusselt number is usually taken to be around 4, cf. [10]. Such a situation is valid for the steady-state, fully-developed laminar flow in blood vessel, which is seldom (if ever) the case.

In the real case, the blood flow is pulsatile and in largest vessels flow reversal may occur [15]. In the terminal arteries, the velocity profiles are closer to the parabolic shape and in the arterioles they characterize a hydrodynamically fully developed flow. Since, according to figure 2 and table 2, these intermediate vessels are most important in the case of the bioheat transfer, it is reasonable to assume a steady-state flow for the purposes of estimating the heat exchange.

The analysis of these effects in a simplified case (straight rigid vessel) was performed in [15]. It consisted of numerical analysis of the coupled momentum and energy equations supplemented with the mass balance equation, under the following assumptions:

1. The blood is assumed to be a Newtonian fluid.

2. The vessels are considered to be rigid.

3. The countercurrent heat exchange is neglected.

4. The vessel wall is assumed to be a perfect thermal sink, i.e. its temperature is constant and higher than the blood temperature.

The results show that the pulsating axial blood velocity produces a pulsating temperature distribution in flowing blood. This effect is negligible in the case of the smallest vessels. It should be noted, however, that the value of through-the-wall heat flux obtained for steady-state flow and the time-averaged value for pulsating flow differ by up to 10% in the terminal arteries [17]. This effect is diminished by increasing the pulsation frequency. In table 4, these differences are specified, see [17]. The blood flow is characterized in terms of the Reynolds number and the Womersley number α defined as follows:

$$Re = \frac{wR}{\nu}, \qquad \alpha = R\sqrt{\omega\nu}\,.$$

Here R is the vessel radius, w denotes the blood time-averaged velocity, whilst ν is the blood kinematic viscosity and ω is the radial frequency of pulsation.

Table 4. Convective heat transfer into a vessel. Differences between numerical steady-state value q_s and the value integrated over one pulsation period q_p, after [17]

Vessel	Reynolds No.	Womersley No.	$(q_p-q_s)/q_s$
Aorta	1667	7.25	– 6.8%
		8.85	– 2.6%
		10.25	+ 9.4%
Large vessels	120	2	– 8.2%
		3	– 7.6%
		4	– 6.3%
Terminal arteries	20	0.6	–10.8%
		0.7	– 8.3%
		0.8	– 7.4%
Arterioles	0.02	0.017	– 3.7%

The results presented in table 4 suggest that the influence of the blood flow pulsation should be accounted for in the theoretical modelling of the bioheat transfer.

3. Soft tissue damage due to hyperthermia

Thermal injury to living cells has been a topic of research for a long time. Its significance has grown with the invention of weapons relying mainly on heat, such as the flame thrower, incendiary charges or napalm and their use in numerous conflicts. The early experimental and theoretical studies were therefore focused mainly on the heat

effect on epidermal injury [25], [26]. The development of various therapeutic techniques relying on the application of elevated temperature to degenerate tissues made considerations of thermal damage mechanisms in other situations necessary.

It has been shown that the dissipation of heat is different in cancerous and in healthy tissues and higher temperature can be attained within tumors. High temperature also has a sensitizing effect in the radiation therapy resulting in better response and longer tumor control with acceptable normal tissue effects, cf. [38] and the references therein.

The thermal treatment of cells leads to numerous degenerative events, but the sequence of events leading to the cellular death still is not well established. Various internal structures of the cell were implicated to be targets of the thermal treatment but none have been proven conclusively to be responsible for cellular death.

The widely-accepted model of thermal damage in a soft tissue is the first-order rate process (the Arrhenius model), cf. [6], [24], [26], [39]. The measure of the injury Ω is introduced and its rate is postulated to satisfy the equation:

$$\frac{d\Omega}{d\tau} = A \exp\left(-\frac{E_a}{BT}\right), \tag{31}$$

where B is the universal gas constant and A, E_a are the frequency constant and the activation energy, respectively; τ denotes the time. The constants A and E_a are model parameters usually obtained experimentally. One can assume that $\Omega = 1$ marks the threshold of irreversible thermal injury that can be detected experimentally. Once this threshold is attained in a given mode of heating after the time τ_A the measured thermal history of the system is used to derive the values of model parameters in accordance with the equation:

$$1 = \int_0^{\tau_A} \exp\left(-\frac{E_a}{BT(\tau)}\right) d\tau \,.$$

For an isothermal regime the time τ_A is simply the reciprocal of the damage rate defined by equation (31). Another way of the normalization is to define Ω in terms of concentrations of the original (native) tissue $C_0(\tau)$ and the damaged tissue $C_d(\tau)$ [13]:

$$\Omega(\tau) = \ln\left(\frac{C_0(0)}{1 - C_d(\tau)}\right), \tag{32}$$

where $C_0(\tau) + C_d(\tau) = 1$ holds for every τ.

There is a wide variety of experimental methods used to identify the time τ_A at which irreversible cellular damage occurs. They rely on different physiological effects and therefore the damage mechanisms to which they react are different. Some methods involve using fluorescent dye markers like propidium iodide, trypan blue or neutral red, which diffuse through heat-damaged cellular membranes. These methods measure essentially cellular membrane damage level which is not necessarily equal to the overall damage measure Ω. Another approach consists in assessing the colony-

forming ability (clonogenics) of the heat-damaged cells after treatment, cf. [6] for details. While this seems to give a good indication of cell viability, the method needs considerable time for post-treatment incubation. In investigations of the viability of the collagenous tissues, the heat-induced shrinkage is usually regarded to be a good, measurable indicator of collagen denaturation, cf. [12], [13], [57].

As can be inferred from table 5 the values of model parameters obtained by using different methods may vary significantly, cf. also [6] and [39] for a comparison. This can give a clue as to what damage mechanisms are responsible for the detected effects. This insight can be gained from the consideration of the activation energy E_a.

Table 5. First-order rate process model of thermal injury parameters (see equation (31)), after [6], [26], [39]

Tissue	Activation energy E_a [kJ/mole]	Frequency factor A [1/s]
Skin	628.5	3.1×10^{98}
Prostrate tumor (clonogenics measurements)	526.4	1.04×10^{84}
Prostrate tumor (propidium iodide uptake measurements)	244.8	2.99×10^{37}
Prostrate tumor (calcein leakage measurements)	81.33	5.069×10^{10}
Arterial tissue	430	5.6×10^{63}
Erythrocyte membrane	212	10^{31}
Hemoglobin	455	7.6×10^{66}
Whole blood	448	7.6×10^{66}

In general, the activation energy of any physical/chemical process is the critical minimum energy that must be possessed by the constituents involved for the process to take place. Therefore the rate of the process will be proportional to the fraction of these constituents which do possess the energy at least equal to the value of the activation energy. This fraction f is deduced from the Maxwell–Boltzman energy distribution law [26]

$$f = \exp\left(-\frac{E_a}{BT}\right). \tag{33}$$

Since the constant E_a in equation (31) can be viewed as the mean activation energy of the physical and chemical processes leading to the heat-induced cellular damage (according to certain experimental criterion), the measured value of this constant, in comparison with the values of activation energy of various well-known processes, provides a foundation for speculations about the mechanisms of cellular injury [6], [26]. HENRIQUEZ [26] divided the potential damage mechanisms into three categories:

(i) *Thermal alterations in proteins*. Proteins contribute to the maintenance of cell life in various ways and undoubtedly even minor heat-induced alterations to these molecules can lead to irreversible damage. Studies on the subject indicate that alterations to proteins occurring in the temperature range of 0–100 °C at measurable rates are not unusual. The activation energy of these processes are often well in excess of

200 kJ/mole and can be strongly dependent on pH. For instance, for the heat denaturation of egg albumin: $E_a = 553$ kJ/mole at pH = 5; for the heat inactivation of invertase $E_a = 461$ kJ/mole at pH = 4 and $E_a = 218$ kJ/mole at pH = 5.7; the hemoglobin: $E_a = 318$ kJ/mole at pH = 5, see [6], [26] and [45]. Experimental studies of isolated rat skeletal muscle reveal that at elevated temperature the rate of protein synthesis increases slightly at first and then falls; simultaneously, the rate of protein breakdown increases steadily [5]. Indeed, the protein balance is changed and loss of body mass may occur even at the temperature range characteristic of fever [5].

(ii) *Other possible alterations in metabolic processes.* This class of effects includes the temperature influence on the kinetics of metabolic processes that do not involve proteins. These are changes in the rates of diffusion, formation and degradation of chemical reactants, etc. The activation energy of these processes is usually of the order of 40–80 kJ/mole. These effects are usually regarded of minor importance to cellular thermal injury as compared to the previous group.

(iii) *Nonprotein-induced alterations in the physical characteristics of cells.* The physical phenomena characteristic of protoplasm but not primarily affected by the thermal alterations of proteins, e.g. diffusion of metabolites through an unaltered cell wall.

The model presented by equation (31) provides a definite connection between the time-temperature history and damage accumulation. It can facilitate design of the hyperthermic treatment procedures allowing for, in principle, accurate damage prediction, provided that the temperature field is known, the model constants are chosen appropriately and the temperature range is suitable. However, it has several shortcomings. For instance, it does not take into account the history of thermal insult, i.e. larger and smaller thermal loads produce the same result, irrespective of their relative order.

The problem not accounted for by the model (31) is the observation that marginally lethal or nonlethal temperatures lead to complete cell destruction, if they are preceded by short preheating at high temperature. Such cells become extremely sensitized to further temperature treatment, which would not otherwise cause death, see [24] for details. This phenomena can be viewed as the considerable lowering of the activation energy E_a by the preheating.

Another issue brought up by experimental investigations is that pH variations may play a similar sensitizing role for some kind of cells, cf. [24], [45] and references therein. It is probable that irradiation, preheating as well as low pH may cripple the cell's capacity to accumulate and/or repair sublethal heat damage which is in turn different for different kinds of cells and may depend on mechanical loading [13]. Surprisingly, the influence of the latter is usually neglected. While *in vitro* tests in thermal baths and on isolated cells yield data usually specific to unloaded specimens, in the clinical *in vivo* experiments the tissue is often loaded in unknown and uncontrollable manner. The investigations of heat-induced shrinkage of collagenous tissue indicate that the increase in the mechanical loading during heating delays the denaturation [13], [20]. Introducing the characteristic time of damage process τ_2 one may write:

$$\tau_2 = \exp\left(\alpha + \beta P + \frac{m}{T}\right),$$

where α, β and m are material coefficients. Scaling the time variable of experimental results (shrinkage measurements) obtained in different temperature-load regimes with τ_2 proved to be an effective way to reduce them to a single master-curve [13], [14], [20], [57].

From a practical point of view it is important to apply the damage measures considered above to the clinical cases, i.e. the hyperthermia protocol design. For this purpose the idea of thermal dose was proposed by SAPARETO and DEWEY [45] and the equivalent time at 43 °C was proposed as a "common denominator" for comparison of thermal treatments. The value of this "break temperature" has been chosen arbitrarily. For a simple case of comparing the two treatments conducted at different temperatures the equivalent time t_{43} is given by:

$$t_{43} = tR^{43-T}, \tag{34}$$

where t is the time of the treatment and T its temperature expressed in °C. The constant R is assumed equal to 0.5 for $T > 43$ °C and $R = 0.25$ for $T < 43$ °C. These assumptions are justified experimentally [45].

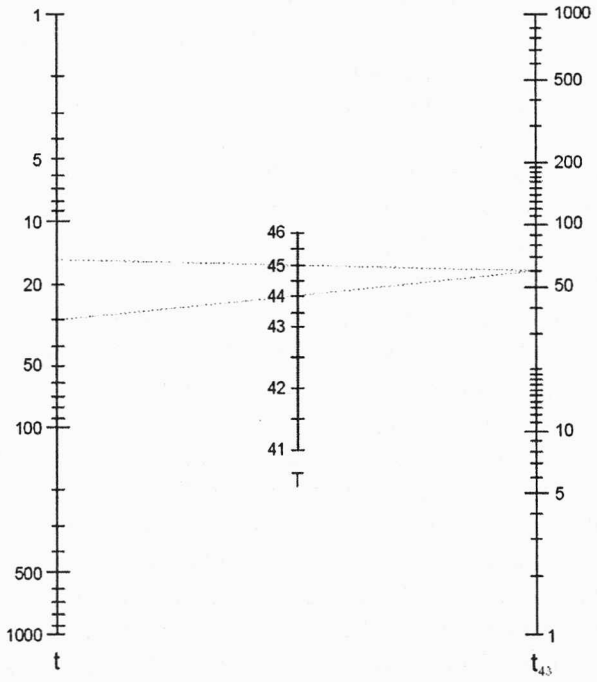

Fig. 9. Nomogram allowing a quick comparison of the isothermal treatments by means of the equivalent time t_{43} at 43 °C. The equivalency of 30-min. treatment at 44 °C and 15-min. treatment at 45 °C is also depicted, after [45]

Criterion (34) is useful only in simple cases of isothermal treatments. For these cases a simple nomogram can be drawn, see figure 9. Unfortunately, the thermal history during hyperthermic treatment is never isothermal. It usually consists of a warming-up period, often exponentially approaching the treatment temperature, the period of approximately constant temperature and the cool-down period. Consequently criterion (34) needs to be extended:

$$t_{43} = \int_0^t R^{43-T(\tau)} d\tau \,. \tag{34}$$

In clinical situation, the temperature profile $T(\tau)$ can be measured with a sufficient accuracy to allow an approximation of the integral in equation (34).

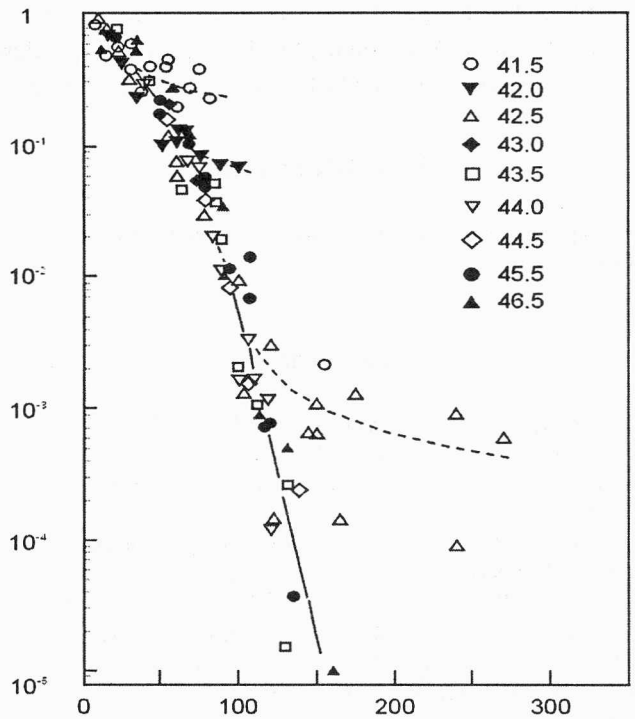

Fig. 10. Surviving fraction of Chinese hamster ovary cells at various temperatures plotted as a function of equivalent minutes at 43 °C. The data for the lowest temperatures deviate from a single line, as shown by the dashed lines, due to development of thermotolerance, after [45]

The concept of equivalent time at 43 °C allows the assessment of the potential threat of the given treatment once the tissue damage is evaluated as a function of treatment time in the experiments conducted at 43 °C. In figure 10, some experimental data are depicted, cf. [45] and the references therein. The deviation of data points for the lowest temperatures in figure 10 from the single line marks the development of thermotoler-

ance. For these temperatures criterion (34) is inadequate as the constant R increases to infinity as the temperature drops to the physiological values. The thermotolerance is partially accounted for by means of the discontinuity of R at 43 °C, but this is by no means satisfactory. The experimental results indicate that cells briefly exposed above 43 °C and then treated below this temperature show no such discontinuity – the effect of thermotolerance is inhibited or delayed. This may be beneficial during hyperthermia treatments since the cells acquire thermotolerance during the warm-up period and are thus less susceptible to damage. Therefore, for the desired therapeutic effect to be attained the treatment needs to be prolonged. The elimination of the unwanted thermotolerance by single high-temperature shock prior to the main treatment could be beneficial. Other means can also be used, e.g. irradiation [45]. More advanced models than (34) are needed to account correctly for phenomenon of thermotolerance.

The investigations of the temperature-induced cell damage in the range of small temperature elevation is important, since long-lasting, small temperature elevations exist in the case of joint articulation due to frictional heating, see Part II of our paper.

Acknowledgement

The authors were supported by the State Committee for Scientific Research (KBN, Poland) through the grant No 8T11F 017 18.

References

[1] BAISH J.W., *Heat transport by countercurrent blood vessels in the presence of an arbitrary temperature gradient*, J. Biomech. Eng., 1990, 112, 207–211.

[2] BAISH J.W., *Formulation of a statistical model of heat transfer in perfused tissue*, J. Biomech. Eng., 1994, 116, 521–527.

[3] BAISH J.W., AYYASWAMY P.S., FOSTER K.R., *Heat transport mechanisms in vascular tissues: a model comparison*, J. Biomech. Eng., 1986, 108, 324–331.

[4] BAISH J.W., AYYASWAMY P.S., FOSTER K.R., *Small-scale temperature fluctuations in perfused tissue during local hyperthermia*, J. Biomech. Eng., 1986, 108, 246–250,.

[5] BARACOS V.E., WILSON E.J., GOLDBERG A.L., *Effects of temperature on protein turnover in isolated rat skelatal muscle*, Am. J. Physiology, 246(1), C125–C130.

[6] BHOWMICK S., SWANLUND D.J., BISCHOF J.C., *Supraphysiological thermal injury in Dunning AT-1 prostrate tumor cells*, J. Biomech. Eng., 2000, 122, 51–59.

[7] BOWMAN H.F., *The bio-heat transfer equation and discrimination of thermally significant vessels*, Annals New York Acad. Sci., 1980, 335, 155–160.

[8] BRINCK H., WERNER J., *Estimation of the thermal effect of blood flow in a branching countercurrent network using a three-dimensional vascular model*, J. Biomech. Eng., 1994, 116, 324–330.

[9] CHARNY C.K., WEINBAUM S., LEVIN R.L., *An evaluation of the Weinbaum–Jiji bioheat equation for normal and hyperthermic conditions*, J. Biomech. Eng., 1990, 112, 80–87.

[10] CHATO J., *Heat transfer to blood vessels*, J. Biomech. Eng., 1980, 102, 110–118.

[11] CHEN M.M., HOLMES K.R., *Microvascular contributions in tissue heat transfer*, Annals New York Acad. Sci., 1980, 335, 137–154.

[12] CHEN S.S., WRIGHT N.T., HUMPHREY J.D., *Heat-induced changes in the mechanics of a collagenous tissue: Isothermal, free shrinkage*, J. Biomech. Eng., 1997, 119, 372–378.

[13] CHEN S.S., WRIGHT N.T., HUMPHREY J.D., *Heat-induced changes in the mechanics of a collagenous tissue: Isothermal, isotonic shrinkage*, J. Biomech. Eng., 1998, 120, 382–388.

[14] CHEN S.S., WRIGHT N.T., HUMPHREY J.D., *Phenomenological evolution equations for heat-induced shrinkage of a collagenous tissue*, IEEE Trans. BME, 1998, 45, (10), 1234–1240.

[15] CRACIUNESCU O.I., CLEGG S.T., *Pulsatile blood flow effects on temperature distribution and heat transfer in rigid vessels*, J. Biomech. Eng., 2001, 123, 500–505.

[16] CRAVALHO E.G., FOX L.R., KAN J.C., *The application of the bioheat equation to the design of thermal protocols for local hyperthermia*, Annals New York Acad. Sci., 1980, 335, 86–97.

[17] CREZEE J., LAGENDIJK J.J.W., *Experimental verification of bioheat transfer theories: Measurement of temperature profiles around large artificial vessels in perfused tissue*, Phys. Med. Biol., 1990, 35, (7), 905–923.

[18] CREZEE J., MOOIBROEK J., LAGENDIJK J.J.W., Van LENEUVEN G.M.J., *The theoretical and experimental evaluation of the heat balance in perfused tissue*, Phys. Med. Biol., 1994, 39, 813–832.

[19] DAVIDSON J.A., GIR S., PAUL J., *Heat transfer analysis of frictional heat dissipation during articulation of femoral implants*, J. Biomed. Mat. Res., 1988, 22, 281–309.

[20] DAVIS E.D., DOSS D.J., HUMPHREY J.D., WRIGHT N.T., *Effects of heat-induced damage on the radial component of thermal diffusivity of bovine aorta*, J. Biomech. Eng., 2000, 122, (3), 283–286.

[21] DILLER K.R., *Modelling of bioheat transfer processes at high and low temperature*, Advances in Heat Transfer, 1992, 22, 177–357.

[22] DURKEE J.W. Jr., ANTICH P.P., LEE C.E., *Exact solutions to the multiregion time-dependent bioheat equation. I: Solution development*, Phys. Med. Biol., 1990, 35, (7), 847–867.

[23] DURKEE J.W. Jr., ANTICH P.P., LEE C.E., *Exact solutions to the multiregion time-dependent bioheat equation. II: Numerical evaluation of the solutions*, Phys. Med. Biol., 1990, 35, (7), 869–889.

[24] HENLE K.J., DETHLEFSEN L.A., *Time–temperature relationships for heat-induced killing of mammalian cells*, Annals New York Acad. Sci., 1980, 335, 234–253.

[25] HENRIQUEZ F.C., MORITZ A.R., *Studies of thermal injury: I. The conduction of heat to and through skin and the temperature attained therein: A theoretical and experimental investigation*, Am. J. Pathology, 1947, 23, 531–549.

[26] HENRIQUEZ F.C. Jr., *Studies of thermal injury: V. The predictability and the significance of thermally induced rate processes leading to irreversible epidermal injury*, Arch. Pathology, 1947, 43, 489–502.

[27] HOFFMANN N.E., BISCHOF J.C., *Cryosurgery of normal and tumor tissue in the dorsal skin flap chamber: Part I. Thermal response*, J. Biomech. Eng., 2001, 123, (4), 301–309.

[28] JAIN R.K., *Temperature distributions in normal and neoplastic tissues during normothermia and hyperthermia*, Annals New York Acad. Sci., 1980, 335, 98–106.

[29] JIJI L.M., WEINBAUM S., LEMONS D.E., *Theory and experiment for the effect of vascular microstructure on surface tissue heat transfer. Part II: Model formulation and solution*, J. Biomech. Eng., 1984, 106, 331–341.

[30] KLINGER H.G., *The description of heat transfer in biological tissue*, Annals New York Acad. Sci., 1980, 335, 133–136.

[31] LAW H.T., PETTIGREW R.T., *Heat transfer in whole-body hyperthermia*, Annals New York Acad. Sci., 1980, 335, 298–310.

[32] LEMONS D.E., CHIEN S., CRAWSHAW L.I., WEINBAUM S., *The significance of vessel size and type in vascular heat transfer*, Am. J. Phys., 1987, 253, R128–R135.

[33] LIU J., *Uncertainty analysis for temperature prediction of biological bodies subject to randomly spatial heating*, J. Biomech., 2001, 34, 1637–1642.

[34] MAJCHRZAK E., JASIŃSKI M., *Sensitivity analysis of bioheat transfer in 2D tissue domain subjected to an external heat source*, Acta Bioengng. Biomech., 2001, 3, 329–336.

[35] MAJCHRZAK E., MOCHNACKI B., *The analysis of thermal processes occurring in tissue with a tumor region using the BEM*, J. Theor. Appl. Mech., 2002, 40, 101–112.

[36] MCHEDLISHVILI G., *Blood flow in the microcirculation is a specific scientific field*, Rus. J. Biomech., 2000, 4, (4), 34–35.

[37] PENNES H.H., *Analysis of tissue and arterial blood temperatures in the resting human forearm*, J. Appl. Physiology, 1948, 1, 93–122.

[38] PEREZ C.A., *Clinical hyperthermia: mirage or reality*? Int. J. Radiation Oncology Biol. Phys., 1984, 10, 935–937.

[39] PFEFER T.J., CHOI B., VARGAS G., Mc NALLY K.M., WELCH A.J., *Pulsed laser-induced thermal damage in whole blood*, J. Biomech. Eng., 2000, 122, 196–202.

[40] RABIN Y., STEIF P.S., *Analysis of thermal stresses around a cryosurgical probe*, Cryobiology, 1996, 33, 276–290.

[41] RABIN Y., STEIF P S., *Thermal stress modeling of the freezing of biological tissue*, Advances in Heat and Mass Transfer in Biotechnology, 1999, 183–187.

[42] RIVOLTA B., INZOLI F., MANTERO S., SEVERINI A., *Evaluation of temperature distribution during hyperthermic treatment in biliary tumors: A computational approach*, J. Biomech. Eng., 1999, 121, 141–147.

[43] ROEMER R.B., CETAS T.C., *Application of bioheat transfer simulations to hyperthermia*, Cancer Res., 1984, 44, 4788s–4798s.

[44] ROEMER R.B., DUTTON A.W., *A generic tissue convective energy balance equation: Part I. Theory and derivation*, J. Biomech. Eng., 1998, 120, 395–404.

[45] SAPARETO S.A., DEWEY W.C., *Thermal dose determination in cancer therapy*, Int. J. Radiation Oncology Biol. Phys., 1984, 10, 787–800.

[46] SHITZER A., STROSCHEIN L.A., VITAL P., GONZALEZ R.R., PANDOLF K.B., *Numerical analysis of an extremity in a cold environment including countercurrent arterio-venous heat exchange*, J. Biomech. Eng., 1997, 119, 179–186.

[47] SONG J., XU L.X., LEMONS D.E., WEINBAUM S., *Enhancements in the effective thermal conductivity in rat spinotrapezius due to vasoregulation*, J. Biomech. Eng., 1997, 119, 461–468.

[48] SONG J., XU L.X., LEMONS D.E., WEINBAUM S., *Microvascular thermal equilibration in rat spinotrapezius muscle*, Annals Biomed. Eng., 1999, 27, 56–66.

[49] SONG W.J., WEINBAUM S., JIJI L.M., LEMONS D., *A combined macro and microvascular model for whole limb heat transfer*, J. Biomech. Eng., 1988, 110, 259–268.

[50] STOLWIJK J.A.J., *Mathematical models of thermal regulation*, Annals New York Acad. Sci., 1980, 335, 98–106.

[51] VALVANO J.W., NHO S., ANDERSON G.T., *Analysis of the Weinbaum–Jiji model of blood flow in the canine kidney cortex for self-heated thermistors*, J. Biomech. Eng., 1994, 116, 201–207.

[52] WEINBAUM S., JIJI L.M., *A new simplified bioheat equation for the effect of blood flow on local average tissue temperature*, J. Biomech. Eng., 1985, 107, 131–139.

[53] WEINBAUM S., JIJI L.M., LEMONS D.E., *Theory and experiment for the effect of vascular microstructure on surface tissue heat transfer: Part I. Anatomical foundation and model conceptualization*, J. Biomech. Eng., 1984, 106, 321–330.

[54] WEINBAUM S., JIJI L.M., LEMONS D.E., *The bleed-off perfusion term in the Weinbaum–Jiji bioheat equation*, J. Biomech. Eng., 1992, 114, 539–544.

[55] WEINBAUM S., XU L.X., ZHU L., EKPENE A., *A new fundamental bioheat equation for muscle tissue: Part I. Blood perfusion term*, J. Biomech. Eng., 1997, 119, 278–288.

[56] WISSLER, E.H., *Comments on the new bioheat equation proposed by Weinbaum and Jiji*, J. Biomech. Eng., 109, 226–233, 1987.

[57] WRIGHT N.T., CHEN S.S., HUMPHREY J.D., *Time–temperature equivalence of heat-induced changes in cells and proteins*, J. Biomech. Eng., 1998, 120, (1), 22–26.

[58] WULFF W., *The energy conservation equation for living tissue*, IEEE Trans. BME, 1974, 21, (6), 494–495.

[59] WULFF W., *Alternatives to the bio-heat transfer equation*, Annals New York Acad. Sci., 1980, 335, 151–154.

[60] ZHU L., LEMONS D.E., WEINBAUM S., *A new approach for predicting the enhancements in the effective conductivity of perfused muscle due to hyperthermia*, Annals Biomed. Eng., 1995, 22, 1–12.

[61] ZHU L., LEMONS D.E., WEINBAUM S., *Microvascular thermal equilibration in rat cremaster muscle*, Annals Biomed. Eng., 1996, 24, 109–123.